ISSN: 2636-8668

Turkish Journal of materials

an international peer-reviewed open access journal

Science Literature
SL PUBLISHING
www.scienceliterature.com

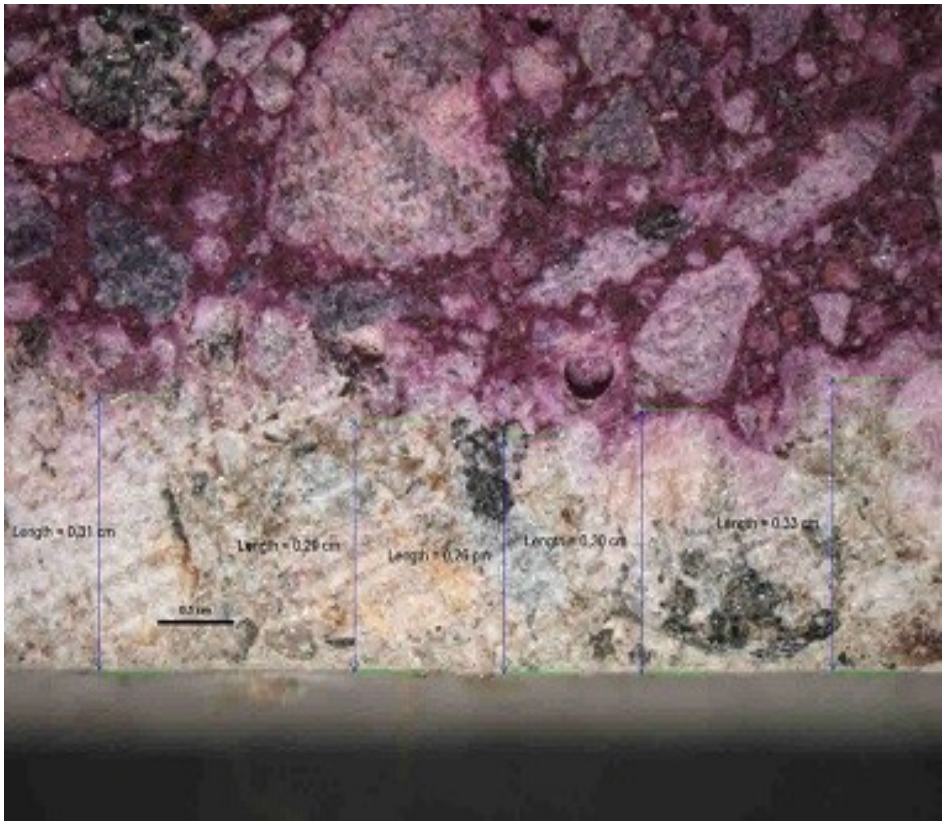

TURKISH JOURNAL OF MATERIALS
VOLUME 3 NO 1

ISSN 2636-8668

2018 January-June Issue

SCIENCE LITERATURE

Kazım Karabekir Work-Center,
F:3/C/196, 50. Year Street,
Lalapaşa Neighborhood,
Yakutiye, Erzurum, Turkey

https://www.scienceliterature.com

09.03.2018

Research Article | Submit Manuscript

Turkish Journal of Materials

Effect of mineral additive use on permeation properties of concrete and the relationship between permeation and carbonation

İlker Ustabaş

Recep Tayyip Erdoğan University, Faculty of Engineering, Department of Civil Engineering, Turkey

Published: 09.03.2018

Turk. J. Mater. Vol: 3 No: 1 Page: 38-52 (2018) ISSN: XXXX-YYYY

SLOI: http://www.sloi.org/sloi-name-of-this-article

*Correspondence E-mail: ilkerustabas@gmail.com

ABSTRACT In this study, effect of fly ash, silica fume and blast furnace slag to the permeation of concrete was investigated. The differences in the absorption, capillary sorption, and ultrasound transmission speed of concrete with and without mineral additives have been studied. Mineral additives have decreased the absorption and sorption of 1-month concrete due to their fine structure by acting as sealant to the pores of concrete. However, when long term (36-month) concrete absorption and sorption is considered, the rate of decrease in permeation of concretes without mineral additives was higher than those with mineral additives because of the effect of carbonation. It was observed that the concrete samples with highest water absorption and capillary water absorption at the 1st month had the lowest water absorption and capillary water absorption at the 36th month. While the permeation of concrete with mineral additives is lower than that of concrete without mineral additives at early-ages (1 month), the permeation of concrete with mineral additives is higher than the concrete without mineral additives at future ages (36 month). The changes in the absorption and sorption of concretes were found to be compatible with the changes in the ultrasound transmission speed.

Keywords: Silica Fume; Fly Ash; Blast Furnace Slag; Capillary; Carbonation; Permeability.

Cite this article: İ. Ustabaş. Effect of mineral additive use on permeation properties of concrete and the relationship between permeation and carbonation. Turk. J. Mater. 3(1) (2018) 38-52.

1. INTRODUCTION

Mineral additives are commonly used in concrete. Mineral addition in concrete and the effect on the properties of concrete is one of the most researched subjects [1-4]. The most preferred mineral additives in concrete include silica fume, fly ash and blast furnace slag [5]. These three are side products of industrial activity and are environmentally hazardous materials, besides they have few application areas apart from concrete sector. Utilization of these at the concrete sector prevents hazard to the environment and enables improvement in properties of concrete as well as cost effectiveness [6,7,8]. Silica fume, fly ash and blast furnace slag, effects fresh and hardened concrete properties such as setting time, consistency, and especially durability [3,7,9]. These are materials which present pozzolanic properties. Pozzolans are materials which do not have self-bonding properties, however, they show bonding ability when mixed with compounds which include calcium. Pozzolans react with CH, formed as a hydration product in fresh concrete, and transforms CH structure into calcium silicate hydrates (CSH). CH has a structure which does not have bonding characteristics and can easily separate from concrete body as a result of external effects. Mineral additions contribute to the durability of concrete via transforming CH structure into CSH structure [10,11].

Concrete is under the influence of degradation mechanisms due to the internal and external media at the environment it is utilized. Intrusion of aggressive ions

from external media into concrete causes degradation. Permeation of concrete has first degree significance in intrusion of hazardous materials, such as carbon-dioxide, chloride and sulfate into concrete [12]. Concrete with low permeation exhibits good performance against chemical degradation mechanisms. Silica fume, fly ash and blast furnace slag decreases the permeation of concrete due to their fine pozzolanic structure [13,14,15]. Permeation of concrete is the main factor in durability of concrete [16,17].

Permeation properties, which include permeability, absorption, diffusivity, capillary etc. [17]. Permeability of concrete may directly be determined by various methods using gas, liquid, chloride or sound waves through concrete. However, permeation of concrete can easily be estimated by measuring its water absorption and capillary water absorption. The use of water absorption and capillary water absorption of concrete is a method which can be applied more easily and quickly than other concrete permeation measurement methods.

Carbonation is another degradation mechanism that damages concrete. Carbon-dioxide in the air reacts with hydration products of concrete and concrete hydration products transform CH and CSH into calcium carbonate [18,19,20].

$$CH+CO2 \rightarrow CaCO3$$

The high alkaline environment in the concrete reduces as a result of carbonation. This phenomenon causes concrete to lose its steel protection characteristic [21]. Another harmful effect of carbonation is to form fractures on concrete [22]. Carbonation is a phenomenon that decreases permeability of concrete. Carbonation may also slightly increase compressive strength of concrete [23]. Mineral additives decrease the permeability of concrete and therefore cause a reduction in carbonation [24]. Permeation of concrete is the main factor in durability of concrete [16,17,25].

The permeation of concrete includes properties such as permeability, absorption, diffusion and capillarity [17,25]. The permeation of concrete is measured by these methods using liquids, gases or chloride ion. The use of water absorption and capillary water absorption of concrete is a method which can be applied more easily and quickly than other concrete permeation measurement methods. Permeation of concrete can easily be estimated by measuring its water absorption and capillary water absorption.

Studies investigating the effect of mineral addition on permeation of concrete indicate that silica fume, fly ash and blast furnace slag reduce the permeation of concrete because of their thin pozzolanic structures [13,14,15,25,26]. Mineral addition reduces the permeation of concrete by filling the pores of both the interface and the bulk phase because of their micro filler structure [15]. In this study, the effect of mineral addition on permeation of concrete in time is investigated. The mineral addition was detected to decrease the permeation of concrete in early ages. The effects of mineral addition on permeation of concrete at later ages were found to be different. The change in the permeation of concrete with mineral addition due to carbonation was determined.

2. EXPERIMENTAL

2.1. Materials

2.1.1. Bonding agents

In this study, CEM I 42,5R class cement has been used. Mechanical and physical properties of bonding agents are shown in Table 1. Chemical compositions of cement, silica fume, fly ash and blast furnace slag are given in Table 2.

2.1.2. Aggregates

Four types of aggregates with their gradation, specific gravity and water absorption values given in Table 3, were mixed together at 10, 15, 25 and 50%, respectively, and were utilized in concrete. Mixture gradation of the aggregate used in the concrete is given in Table 3.

2.2 Concrete design and production

Six groups of concrete were produced within the context of the study. NC-1 and NC-2 concretes were produced without mineral addition. In NC-1 and NC-2 concretes, 300 and 360 kg cement per m3 were used, respectively as given in Table 4. SFC-1 and SFC-2 series concretes had silica fume addition. SFC-1 concretes were produced by using 300 kg cement and 60 kg silica fume per m3 concrete. SFC-2 series concretes were produced by adding 36 kg of silica fume to 324 kg of cement. Concretes with fly ash addition (FAC) and blast furnace slag addition (BFSC) have been produced by adding 60 kg of fly ash and blast furnace slag to 300 kg cement. Concretes were designed for water/bonding agent ratio to be 0.5 in NC-2, SFC-1, SFC-2, FAC and BFSC concretes, and 0.6 in NC-1 concretes.

Concretes were mixed in a mixer of 120-liter capacity. Concrete samples were molded by a single person in a manner to avoid segregation. A total of 32 cubic concrete samples with 15 cm dimensions were obtained from a single concrete mixture. A total of 192 cubic samples having 15 cm dimensions were produced in six runs.

2.3. Water absorption and capillary water absorption

Concrete samples were placed in water for 48 hours before water absorption and capillary water absorption experiments. Then the samples were taken out of water, water film on the surface of the concretes was cleaned and their wet mass was weighed. The air-dried mass of the samples was weighed after they were dried at ambient temperature. After the samples were air-dried, they were dried at oven at 70ºC until they reach a constant mass and then their dry mass was weighed. The cubic samples having 15 cm dimensions were coated with paraffin by leaving the bottom 3 cm open. The remaining uncoated concrete surface was placed in water, and capillary water absorption amounts at 1st, 2nd, 4th, 6th, and 24th hours were determined. The water absorption amount of concretes per unit area (Q) was plotted against the square root of elapsed time ($\sqrt{t}$) and a simple linear regression analysis was used to determine the equation of the line according to the relation: $Q=k.\sqrt{t}$. Capillary water absorption coefficients of concretes were then computed from the slope of that line.

Water absorption values of concretes were determined by subtracting the dry mass from air-dried mass and dividing this by the dry mass.

2.4. Compressive strength, tensile strength, ultrasound transmission rate and surface hardness of concrete

After a standard cure of 28 days was applied to the concrete, the 28-day compressive strength, tensile strength, ultrasound transmission rate, surface hardness, water absorption and capillary water absorption values of concretes were measured. Compression test and tensile strength test were applied to three samples each from every concrete series. Ultrasound transmission rate and surface hardness (via impact testing hammer), were measured from six samples used in determining the compressive and tensile strength of the concretes. If there was a sample deviating considerably from the average during the tests, the value acquired from this sample was omitted and a value acquired from an auxiliary sample was utilized in the determination of an average value. After the first month test, the remaining samples were left in an environment with a moisture changing between 40 and 80% and a temperature ranging between 0 and 30°C. Compressive strength, splitting tensile strength, ultrasound transmission rate and surface hardness of concretes were measured at 10th and 36th months. Surface hardness of concretes was measured with a Schmidt hammer. A total of 12 measurements, using the Schmidt hammer, were taken from each concrete sample and total of 10 surface hardness measurements were taken into consideration by omitting the highest and lowest values. After ultrasound transmission rates and surface hardness of the samples were determined using the Schmidt hammer, compressive and splitting tensile strengths of the same samples were determined. Surface hardness, compressive strength and splitting tensile strength tests were performed in accordance with the TS EN 12504-2, TS EN 12390-3 and TS EN 12390-6 standards, respectively [27,28,29].

2.5. Measurement of carbonation thickness

By using the specimen cutting machine, three pieces having approximately 1 cm thickness were cut from each group of three cubic samples with 15 cm dimensions, Surface of these samples were washed and cleaned. Phenolphthalein was applied with a brush on the surfaces of the concrete samples which were air-dried for 24 hours. While the color of the locations where carbonation occurred did not change on the phenolphthalein applied surfaces of the concrete, the color of the remaining area changed into a pinkish hue (Figure 1). Concrete surfaces were examined with a Nikon SMS 1000 type microscope and edges with carbonation were photographed. Closely spaced measurements were taken at three edges of concrete with NIS Element computer software (Figure 2). Average of these measurements was recorded as carbonation thickness.

Microstructural examination with a scanner electron microscope (SEM) and elemental analysis by spectral analysis (EDS) were conducted on the samples taken from the edges and the middle section of the concretes in order to investigate the carbonation event on the edge and inside the concretes.

3. RESULTS

Table 5 shows compressive and splitting tensile strength of the concrete groups in 1st, 10th, and 36th months. Each value in Table 5 is the average of strength tests of the three cubic concrete samples of 150x150x150 mm dimensions. Figure 3 shows that the highest 1-month compressive strength is observed in SFC-1 series concretes and the lowest 1-month compressive strength is observed in NC-1 series concretes. Compressive strengths of the other concrete groups were ordered from highest to lowest as BFSC, NC-2, SFC-2 and FAC. The order of the compressive strengths of concretes at 10th and 36th months are the same as in the 1st month. Compressive strength of the concretes at 10th month has increased 27% in FAC group and approximately 20% in the remaining groups in comparison to the values in the 1st month. Compressive strength of the concretes was increased by a small amount from 10th to 36th month. It can be seen from Figure 4 that splitting tensile strength of the concretes are not in order similar to the change in compressive strength shown in Figure 3. However, it is understood from Figure 4 that, concretes which have high compressive strength have high splitting tensile strengths as well.

Surface hardness and ultrasound transmission rates of concretes are shown in Table 6. Each value in Table 6 is the average of the values acquired from six concrete samples. Figure 5 shows the variation of surface hardness of concretes at 1st, 10th and 36th months. The highest surface hardness at 1st month was determined in BFSC concrete which have furnace slag addition. The surface hardness of concretes has increased approximately 15% from 1st month to 10th month. No distinct change was observed in the surface hardness of concrete samples between 10th and 36th months, except NC-1 and NC-2 series. Surface hardness of NC-1 series concretes has increased approximately 3% from 10th month to 36th month. Although the surface hardness of NC-2 concretes were lower than that of BFSC in the 1st month, the surface hardness of NC-2 concretes were higher in the 36th month. Carbonation may have affected the changes in surface hardness of NC-1 and NC-2 samples. Ultrasound transmission rates of concretes are shown in Figure 6. The ultrasound transmission rates of all concrete groups were observed to increase from the 1st month to the 10th month. It can be seen from Figure 6 that the ultrasound transmission rates in the 36th month are close to those of the 10th month.

Table 7 shows the capillary water absorption coefficient and water absorption values of the concretes. Values presented in Table 7 have been calculated from three 15 cm cubic concrete samples for each concrete group. Figures 7 and 8 show that NC-1 group concretes have the highest capillary water absorption coefficient as well as the highest water absorption value in the 1st month. NC-1 group concretes are followed in decreasing order by NC-2, FAC, SFC-2, BFSC and SFC-1 type concretes. These findings indicate that, mineral addition decreases the 1st month permeability of concrete. Figures 8 and 9 show that the capillary water absorption and water absorption values of all concrete series were decreased from the 1st month to the 36th month. SFC-1 concretes which have the lowest water absorption and capillary water absorption in the 1st month have the highest water absorption and capillary water absorption value in the 36th month. It can be observed that the order in the values of capillary water absorption and water absorption of all concrete groups in the 1st month is reversed in the 36th month. In other words, the concrete with the highest water absorption and capillary water absorption at the 1st month has the lowest water

absorption and capillary water absorption at the 36th month. When concretes with and without mineral additives are compared, it can be seen that mineral addition decreases the 1-month concrete permeation whereas increases the 36-month concrete permeation. Kockal [26] indicated that mineral additives decrease the permeation of concrete at initial times for 1-year concretes; however, they have no effect on permeation over the long term. The reason for this situation is understood in this study. The permeation of all concretes was equal one year later because the rate of decrease in permeation of concrete due to carbonation in concretes with high permeation is higher than in the concretes with mineral addition. Had they considered longer durations, Kockal [26] could have determined the permeation values of concrete with and without mineral addition found in this study. Figures 9 and 10 show how capillary water absorption coefficient of 1-month and 36-month concretes of NC-1 series was calculated with simple linear regression equation and specificity coefficient. In Figure 10, it can be seen that capillary absorbed water amount vs. square-root of time curve transforms into a decreasing curve.

It was observed that, the ratio of capillary water absorption coefficient to water absorption value in the 1st month, for a concrete in the same concrete group, is very close to the ratio of capillary water absorption coefficient to water absorption value in the 36th month. The reduction in capillary water absorption coefficient of the concretes is similar to the decrease in water absorption values. The concretes with low water absorption values also have a low capillary water absorption coefficient (Figures 7 and 8).

The carbonation thicknesses measured at 36-month concretes are shown in Table 8. In Figure 11, it is seen that the highest carbonation is at NC-1 group concretes and it is followed by NC-2, FAC, SFC-2, BFSC and SFC-1 type concretes. The same order, from highest to lowest, may also be observed in capillary water absorption and water absorption values of the 1-month concretes. Higher carbonation rates were observed at the concretes with high permeability at the 1st month. It is understood that carbonation is the reason for decrease in capillary water absorption and water absorption values of concretes from the 1st month to the 36th month. Carbonation development rate have changed according to the permeation of concrete at early-ages. The mineral additives which decreased the permeability of concrete at early ages have also decreased the carbonation amount as well. Mineral additives in concrete cause transformation of CH into CSH, and the decrease in the CH amount may decrease the development rate of carbonation in these concretes. Increase of carbonation thickness at the concretes with faster carbonation development has caused a decrease of capillary water absorption coefficient and water absorption coefficient of the concrete. This phenomenon has caused the concretes with highest permeation in the 1st month to have the lowest permeability in the 36th month.

XRD analysis was performed on the grinded samples acquired from the carbonated edge of the 36-month concrete samples. Diffraction curves of X-Ray diffraction (XRD) analyses can be seen in Figures 12-17. It is observed that the XRD analyses of six concretes are similar to each other. Dominant peak was observed for quartz and calcium aluminum silicate, while calcium carbonate and portlandite can be observed in lower peaks.

Cubic concrete pieces of NC-1 series with approximately 3mm side length were cut from the carbonated edges and also from the center sections not affected from the carbon dioxide of air. These concrete pieces were coated with gold while vacuumed and then inspected by electron microscope (SEM). Figures 18 and 19 show the results of SEM analysis. Spectral analysis (EDS) was performed on NC-1 series concrete with SEM. Tables 9 and 10 present the elements and ratios determined by EDS. Tables 9 and 10 show that the amount of carbon at the edges where carbonation occurred is higher than the center sections.

The relationship between the carbonation determined in concrete and the permeation is examined microstructurally by XRD analysis and SEM. Similar formations were detected by XRD analysis and SEM images in all concretes. SEM images and spectral analysis revealed an idea about carbonation however a relationship between carbonation and permeation could not be discovered.

4. CONCLUSION

Mineral additives decrease the permeation of concrete with their fine structures and pozzolanic properties. They also affect the strength of concrete via transforming CH structure into CSH structure. At initial ages, (1st month) permeability of the concretes with mineral additives is lower than concretes without mineral additives. At later ages (36th month) permeation of the concretes with mineral additives becomes higher than that of concretes having no mineral additives. While mineral additives decrease the permeability of concrete at initial stages, they cause the permeability of concretes to become higher at later stages when compared to concretes without mineral addition. Carbonation develops slowly at the concretes with mineral addition having low permeability and CH. On the other hand, high permeability and CH increases carbonation in concretes without mineral addition. Carbonation acts to decrease the permeation. At later ages, permeation of concrete without mineral addition is lower due to thicker carbonation development when compared to concrete with same properties but with mineral addition.

The permeation of concrete without mineral addition is lower at the end of 3 years. Less permeation in concrete with mineral addition causes less carbonation. Even if the permeation at the end of three years is lower, the rate of decrease in the permeation of concrete without mineral addition is higher. The permeation of concrete at the end of 3 years is sorted the opposite of the permeation at the end of 1 month.

References

[1] A.D. Aydin, R. Gül, Influence of volcanic originated natural materials as additives on the setting time and some mechanical properties of concrete, Construction and Building Materials 21 (2007) 1277–1281.

[2] S.A. Barbhuiya, J.K. Gbagbo, M.I. Russell, A.M. Basheer, Properties of fly ash concrete modified with hydrated lime and silica fume, Construction and Building Materials 23 (2009) 3233–3239.

[3] T. Nochaiya, W. Wongkeo, A. Chaipanich, Utilization of fly ash with silica fume and properties of Portland cement–fly ash–silica fume concrete, Fuel 89 (2010) 768–774.

[4] O. Kayali, B. Zhu, Corrosion performance of medium-strength and silica fume high-strength reinforced concrete in a chloride solution, Cement & Concrete Composites 27 (2005) 117–124.

[5] M. Mazloom, A.A. Ramezanianpour, J.J. Brooks, Effect of silica fume on mechanical properties of high-strength concrete, Cement & Concrete Composites 26 (2004) 347–357.

[6] X. Pu, Investigation on pozzolanic effect of mineral additives in cement and concrete by specific strength index., Cement and Concrete Research, 29(1999) 951–955.

[7] M. Şahmaran, H.A. Christianto, Ö. Yaman, The effect of chemical admixtures and mineral additives on the properties of self-compacting mortars, Cement & Concrete Composites 28 (2006) 432–440.

[8] H. Yazıcı, The effect of silica fume and high-volume Class C fly ash on mechanical properties, chloride penetration and freeze–thaw resistance of self-compacting concrete, Construction and Building Materials 22 (2008) 456–462.

[9] X.Y. Wang, H.S. Lee, Modeling the hydration of concrete incorporating fly ash or slag, Cement and Concrete Research 40 (2010) 984–996.

[10] I.L. Müller, Influence of silica fume addition on concretes physical properties and on corrosion behaviour of reinforcement bars., Cement & Concrete Composites 26 (2004) 31–39.

[11] H.W. Song, S.W. Pack, J.C. Nam, V. Saraswathy, Estimation of the permeability of silica fume cement concrete, Construction and Building Materials 24 (2010) 315–321.

[12] J. Skalny, J. Marchand, I. Odler, Sulfate Attack on Concrete, Spon Press, New York (2002).

[13] H.W. Song, J.C. Jang, V. Saraswathy, K.J. Byun, An estimation of the diffusivity of silica fume concrete, Building and Environment 42 (2007) 1358–1367.

[14] M.S. Ahmed, O. Kayali, W. Anderson, Chloride penetration in binary and ternary blended cement concretes as measured by two different rapid methods, Cement & Concrete Composites 30 (2008) 576–582.

[15] C. Taşdemir, Combined Effect of Mineral Admixtures and Curing Conditions on the Sorptivity Coefficienty of Concrete, Cement and Concrete Research, 33 (2003) 1637-1642.

[16] D.P. Bentz, Influence of silica fume on diffusivity in cement-based materials II. Multi-scale modeling of concrete diffusivity. Cement and Concrete Research 30 (2000) 1121–1129.

[17] W. Zhu, J.M. Bartos, Permeation properties of self-compacting concrete, Cement and Concrete Research, 33 (2003) 921-926.

[18] K.Y. Ann, S.W. Pack, P.P. Hwang, H.W. Song, S.H. Kim, Service life prediction of a concrete bridge structure subjected to carbonation, Construction and Building Materials 24 (2010) 1494–1501.

[19] B. Johannesson, P. Utgenannt, Microstructural changes caused by carbonation of cement mortar, Cement and Concrete Research 31 (2001) 925–931.

[20] X.Wang, H.A. Lee, model for predicting the carbonation depth of concrete containing low-calcium, fly ash, Construction and Building Materials, 23 (2009) 725-733.

[21] C.H. Chang, J.W. Chen, The experimental investigation of concrete carbonation depth, Cement and Concrete Research 36 (2006) 1760–1767.

[22] H.W. Song, S.J. Kwon, K.J. Byun, C.K. Park, Predicting carbonation in early-aged cracked concrete, Cement and Concrete Research 36 (2006) 979–989.

[23] W.A. Klemm, R.L. Berger, Accelerated curing of cementitious systems by carbon dioxide: part I. Portland cement. Cement and Concrete Research; 2(5) (1972) 567–576.

[24] M.P. Kulakowski, F.M. Pereira, D.C.C. Dalmolin, Carbonation-induced reinforcement corrosion in silica fume concrete, Construction and Building Materials;23(3) (2009) 1189–1195.
E.K.K. Nambiar, K. Ramamurthy, Sorption characteristics of foam concrete, Cement and Concrete Research 37 (2007) 1341– 1347.

[25] U.N. Kockal, F. Türker, Effect of environmental conditions on properties of concretes with different cement types, Construction and Building Materials, 23 (2009) 1862-1870.

[26] TS EN 12390-3, Testing hardened concrete, Compressive strength of test specimens, Standard, (2010).

[27] TS EN 12390-6, Testing hardened concrete, Tensile splitting strength of test specimens, Standard, (2010).

[29] TS EN 12504-2, Testing concrete in structures, part-2 non-destructive testing, determination rebound number, Standard, (2004).

Figures

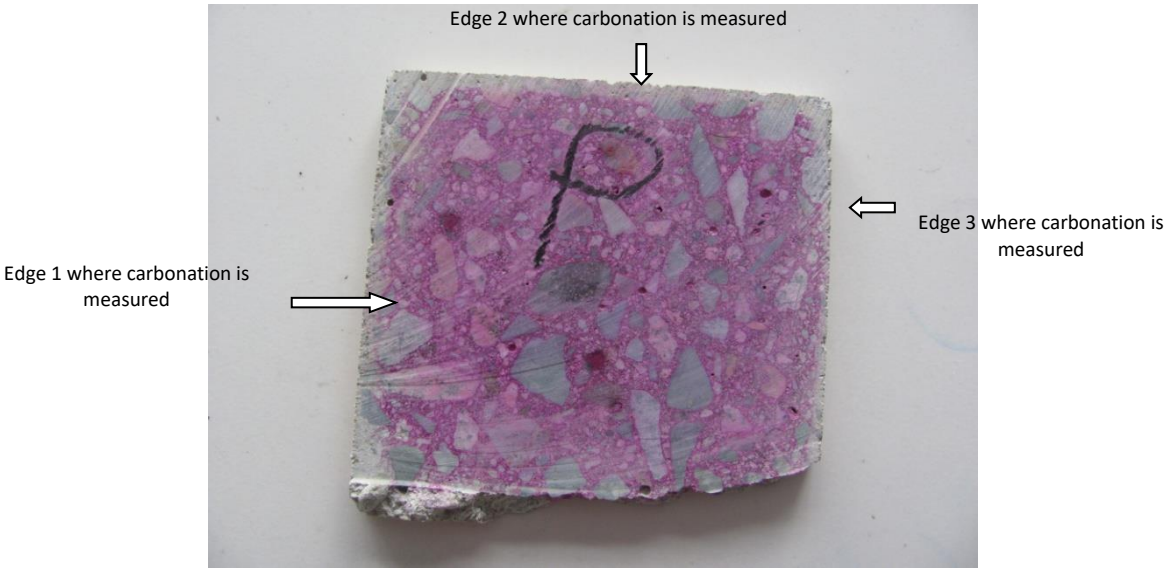

Figure 1. *View of the concrete obtained from cubic concrete sample of 15 cm dimensions by cutting and on what carbonation formation occurred at the edges after phenolphthalein is applied (NC-1).*

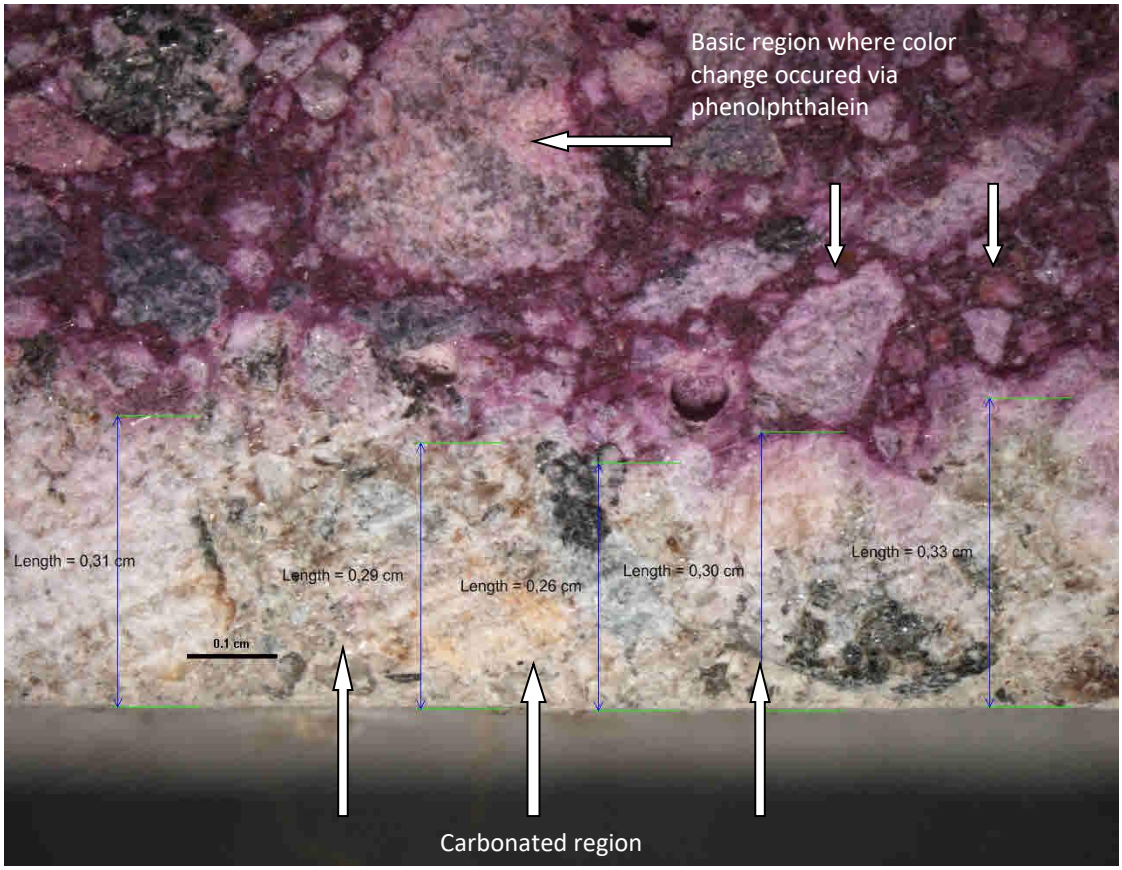

Figure 2. *Measurement of carbonation thickness.*

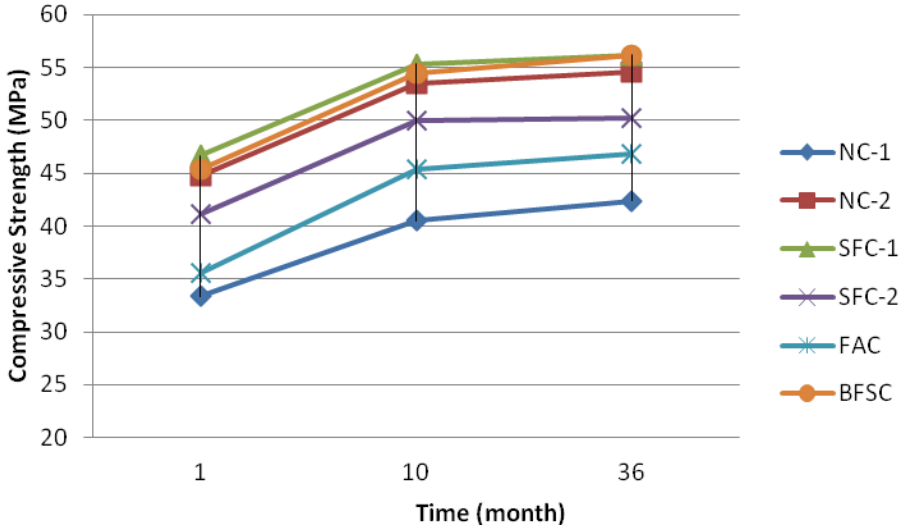

Figure 3. *Compressive strengths of the concretes at months 1, 10 and 36.*

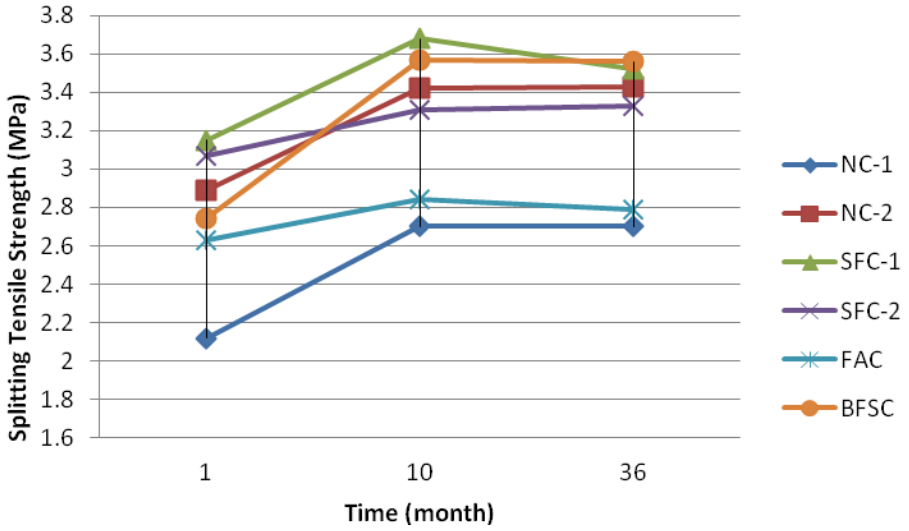

Figure 4. *Splitting tensile strengths of the concretes at months 1, 10 and 36.*

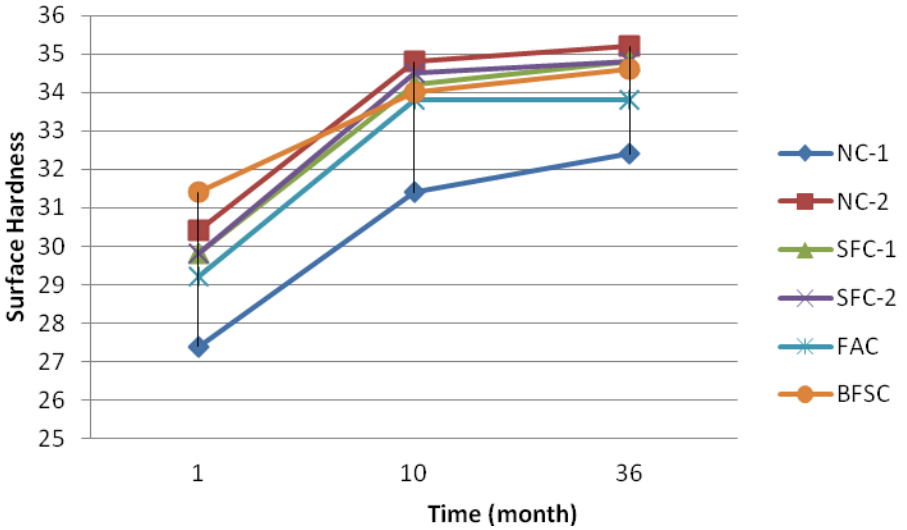

Figure 5. *Surface hardness's of the concretes at months 1, 10 and 36.*

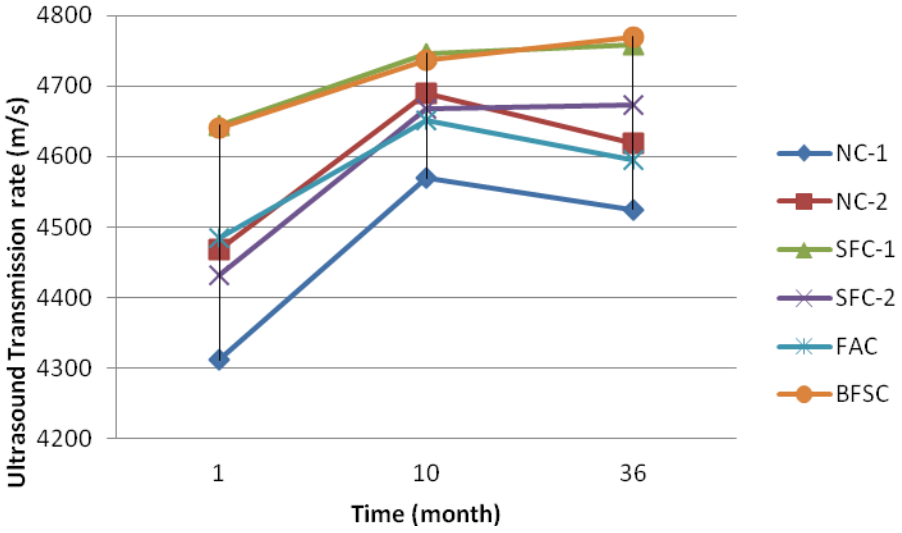

Figure 6. *Ultrasound transmission rates of the concretes at months 1, 10 and 36.*

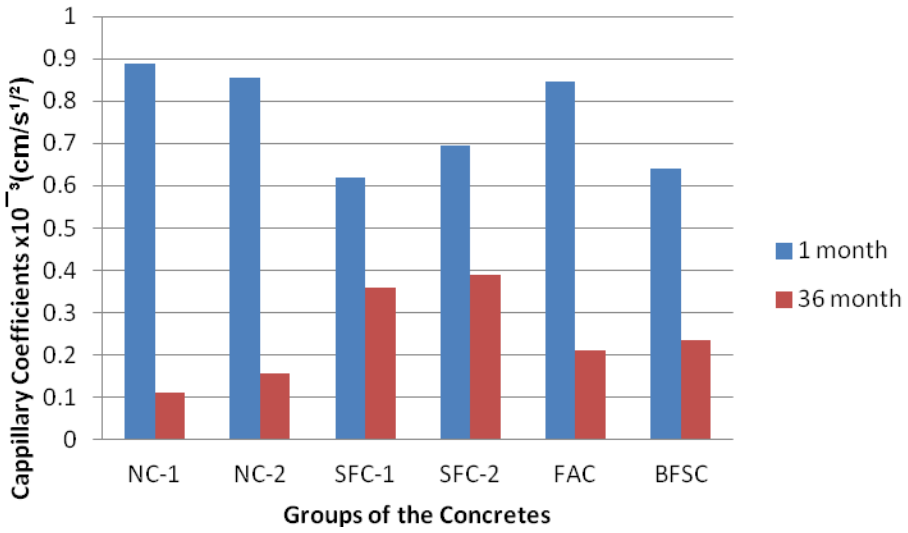

Figure 7. *Capillary water absorption coefficients of the concretes groups at months 1 and 36 (cm/s$^{1/2}$).*

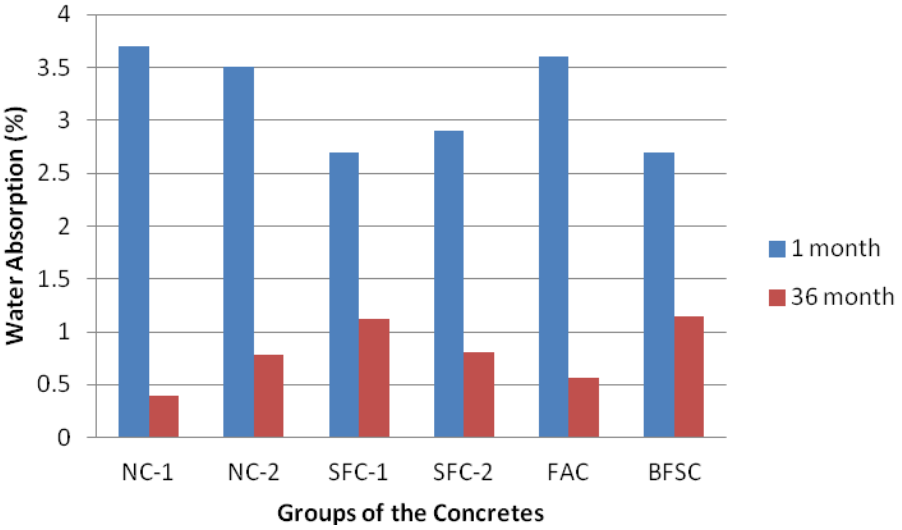

Figure 8. *Water absorption values of the concrete groups at months 1 and 36 (%).*

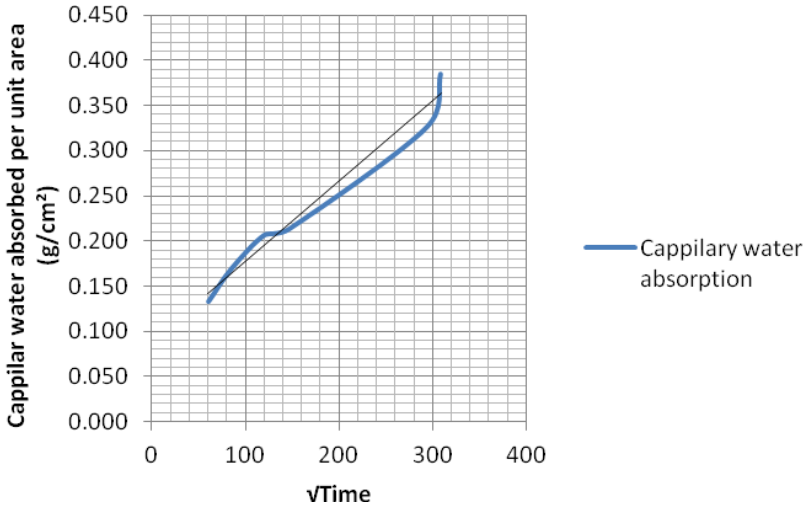

Figure 9. *Capillary water absorption simple regression equation and coefficient of determination for NC-1 concretes at month 1.*

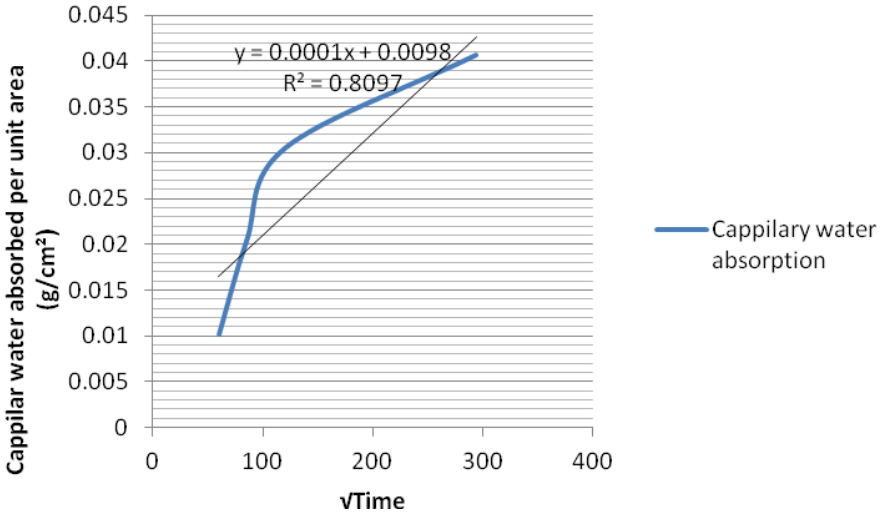

Figure 10. *Capillary water absorption simple regression equation and coefficient of determination for NC-1 concretes at month 36.*

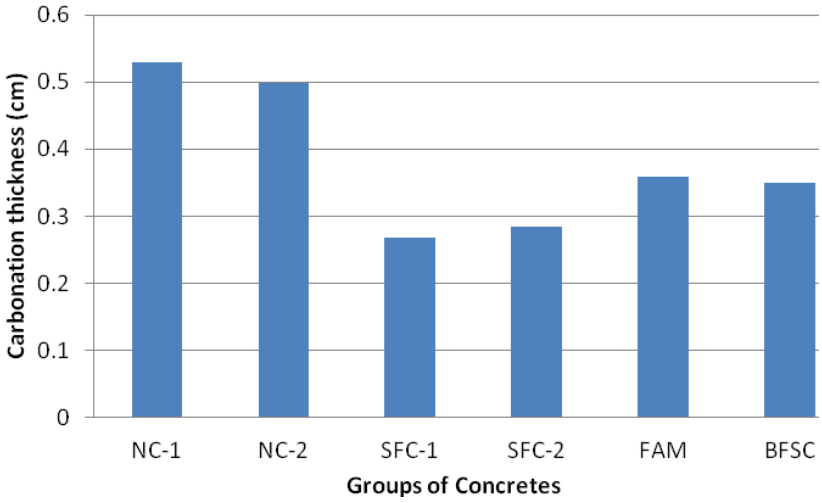

Figure 11. *Carbonation thicknesses of the concretes.*

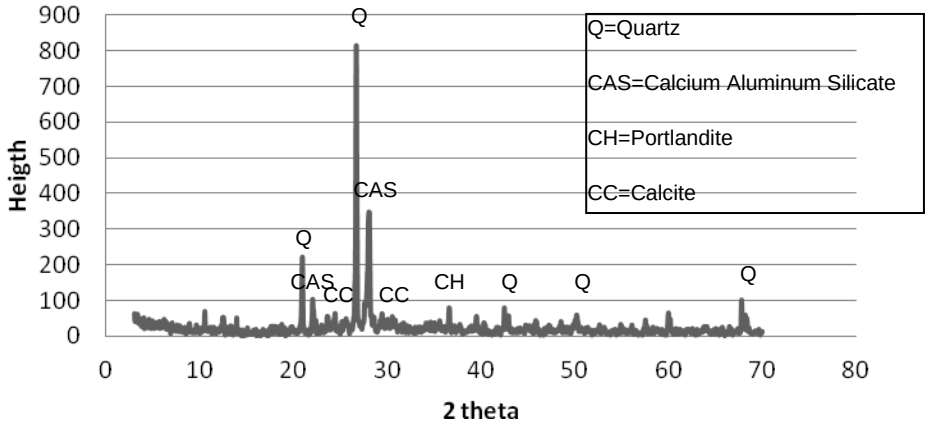

Figure 12. *XRD diffractogram of NC-1 concrete.*

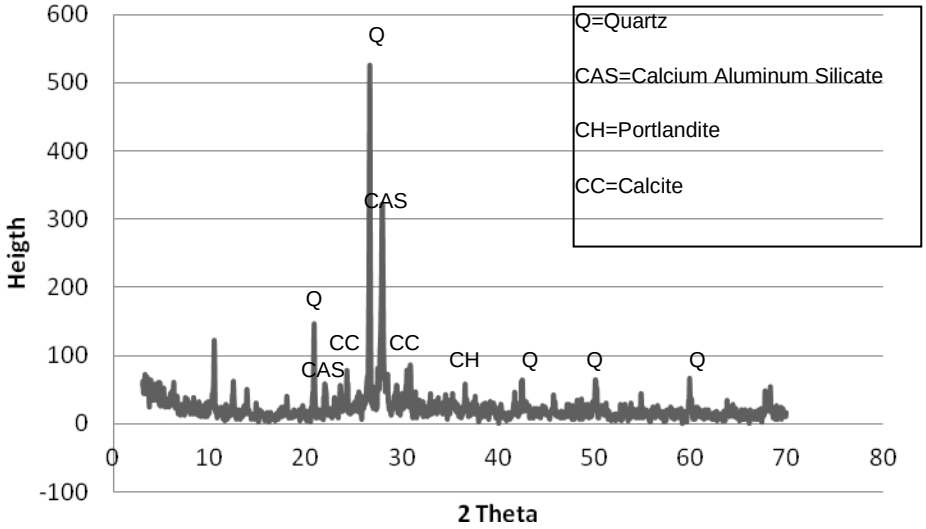

Figure 13. *XRD diffractogram of NC-2 concrete.*

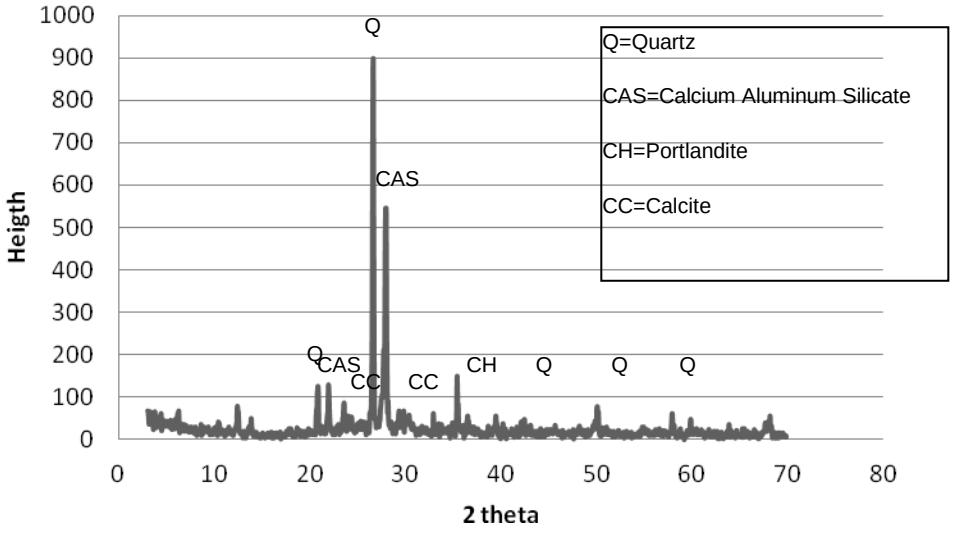

Figure 14. *XRD diffractogram of SFC-1 concrete.*

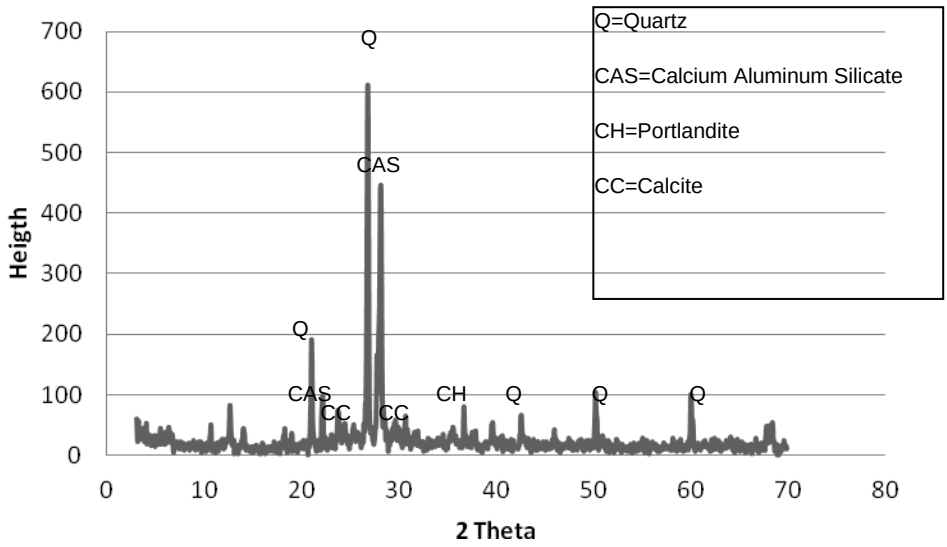

Figure 15. *XRD diffractogram of SFC-2 concrete.*

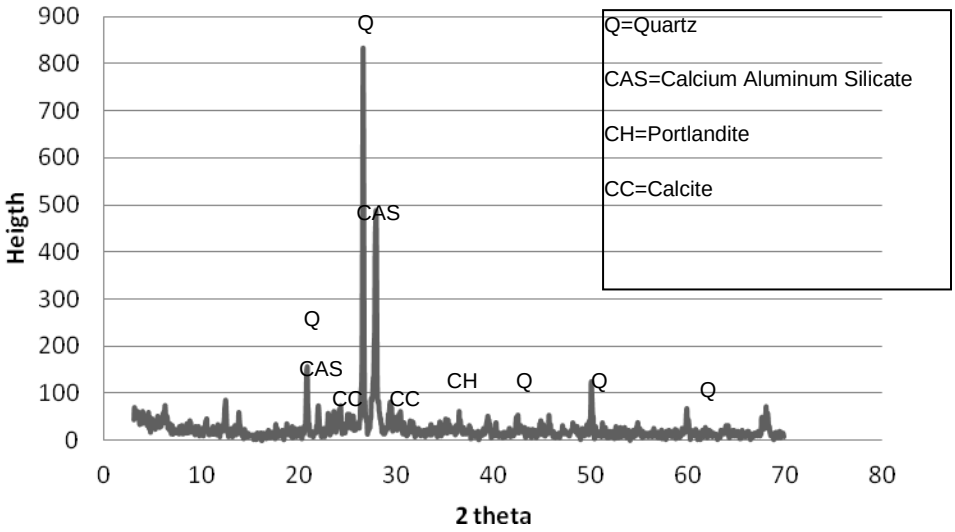

Figure 16. *XRD diffractogram of FAM concrete.*

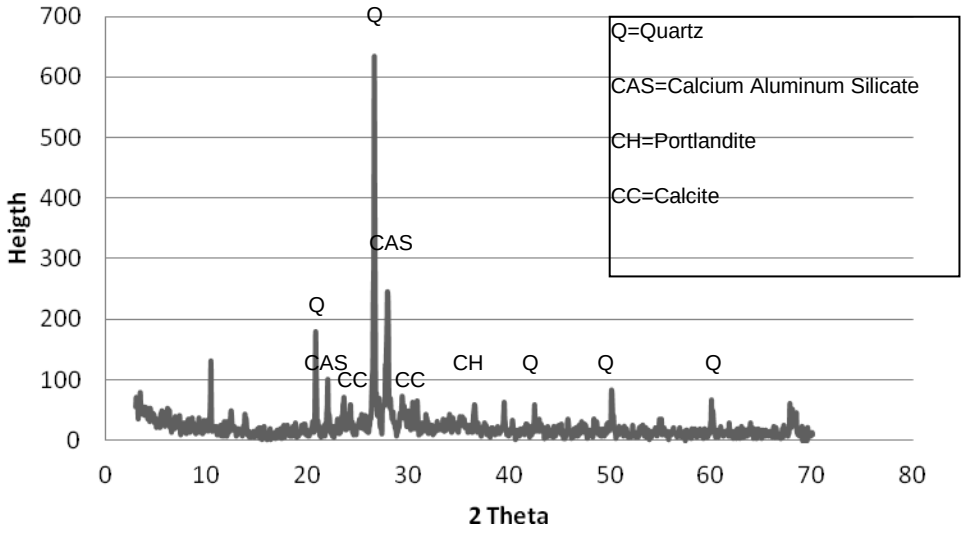

Figure 17. *XRD diffractogram of BFSC concrete.*

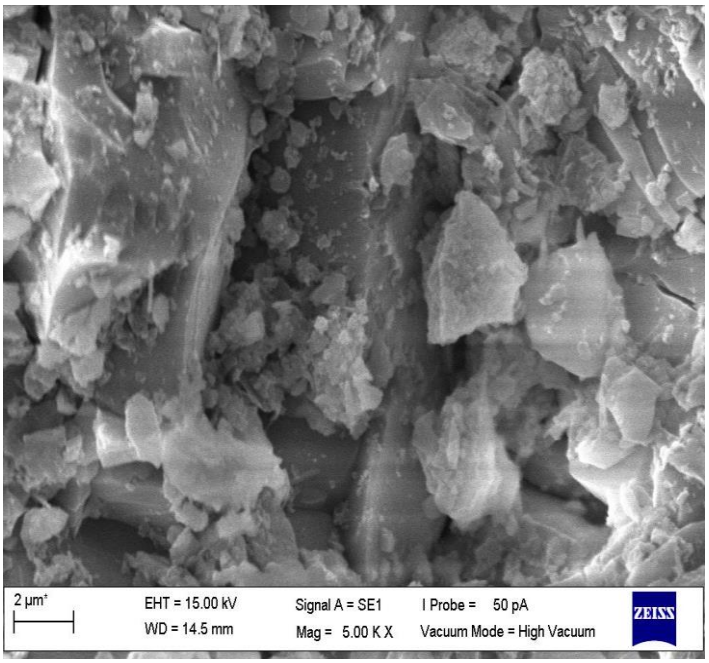

Figure 18. *SEM micrograph of the edge of NC-1 concrete (SEM 1x5000).*

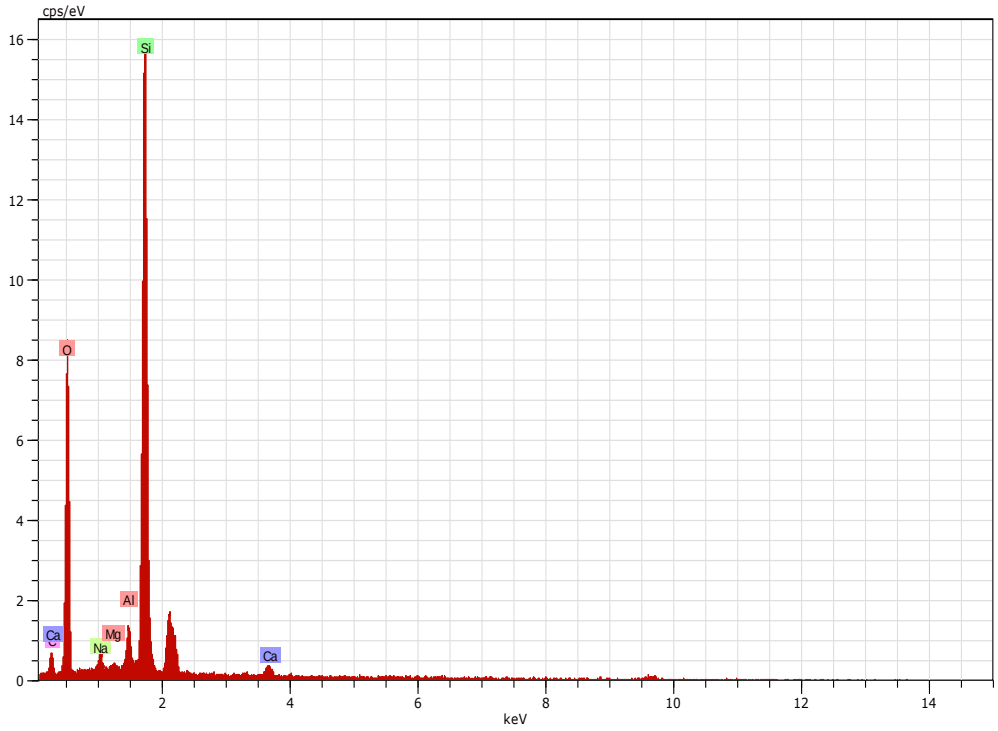

Figure 19. *EDS spectra of the edge of NC-1 concrete.*

Tables

Tablo 1. *k_1 ve n sayısı için değerler*

	XC1	XC2	XC3	XC4
k_1	1	0.20	0.77	0.41
n	0	0.183	0.02	0.085

Table 2. *Mechanical and physical properties of cement, silica fume, fly ash and blast furnace slag.*

Bonding Agents		Cement	Silica Fume	Fly Ash	Blast Furnace Slag
Specific weight		3.05	2.2	2.4	2.7
Specific surface (cm^2/g)		3832	200000	4220	4450
Flexural (Buckling) strength N/mm^2	2 days	5.02			
	28 days	8.18			
Compressive strength N/mm^2	2 days	25.9			
	28 days	46.3			

Table 3. *Chemical properties of the bonding agents.*

Chemical composition (%)	Cement	Silica Fume	Fly Ash	Blast Furnace Slag
CaO	54.7	0.5	1.3	25.3
SiO_2	24.9	95.3	57	43.3
Al_2O_3	5.3	0.7	1.1	13.6
Fe_2O_3	3	0.9	4.3	0.3
MgO	1.6	1.4	16.3	10.5
SO_3	3.3	0.4	0.4	3.7
Na_2O	0.9	0.3	0.4	0.2
K_2O	1.1	0.8	2.9	1.1
Cl^-	0.004	0.1	0.05	0

Table 4. *Properties of aggregate.*

Aggregate type	Aggregate % passing Sieve Size (mm)								Specific weight	Water absorption
	31.5	16	8	4	2	1	0.5	0.25		
Crushed rock (I)	100	10	1	0	0	0	0	0	2.73	1.02
Crushed rock (II)	100	59	1	1	0	0	0	0	2.73	1.14
Crushed rock (III)	100	100	56	10	5	2	2	1	2.72	1.46
Natural sand	100	100	100	97	70	22	22	10	2.62	2.3
Aggregate mixture	100	85	64	51	36	12	12	5		

Table 5. *Concrete mixture ratios and properties of fresh concrete.*

Concrete Group		NC-1	NC-2	SFC-1	SFC-2	FAC	BFSC
Water/ Bonding Agent ratio		0.6	0.5	0.5	0.55	0.5	0.5
Cement (kg/m^3)		300	360	300	324	300	300
Water (kg/m^3)		180	180	180	180	180	180
Mineral additives (kg/m^3)		0	0	60	36	60	60
Super plasticizer (kg/m^3)		3.6	3.6	3.6	3.6	3.6	3.6
Aggregates	I	186	188	189	186	187	187
	II	279	282	284	280	281	281
	III	481	468	472	465	466	466
	sand	928	902	910	896	899	899
Slump (mm)		12	10	7	9	12	12
Density (kg/m^3)		2296	2335	2308	2322	2227	2325

Tablo 6. *The temperature and humidity condition of the room where the concrete samples are stored.*

Aylar	Ocak	Şubat	Mart	Nisan	Mayıs	Haziran	Temmuz	Ağustos	Eylül	Ekim	Kasım	Aralık
En düşük sıcaklık	11	10	14	15	17	20	22	22	20	18	14	12
En yüksek sıcaklık	21	22	24	24	25	26	30	29	24	23	23	22
% Nem (ortalama)	32	34	42	46	58	66	84	72	56	48	36	36

Table 7. *Compressive and splitting tensile strengths of the concretes.*

Concrete Groups	Compressive strength (N/mm^2)			Splitting Tensile strength (N/mm^2)		
	Month 1	Month 10	Month 36	Month 1	Month 10	Month 36
NC-1	33.38	40.53	42.36	2.12	2.7	2.7
NC-2	44.82	53.42	54.63	2.89	3.42	3.43
SFC-1	46.66	55.32	56.14	3.15	3.68	3.52
SFC-2	41.19	49.93	50.16	3.07	3.31	3.33
FAC	35.54	45.40	46.83	2.63	2.84	2.79
BFSC	45.36	54.43	56.16	2.74	3.57	3.56

Table 8. *Surface hardness's and ultrasound transmission rates of the concrete samples.*

Concrete Groups	Surface Hardness			Ultrasound transmission rate (m/s)		
	Month 1	Month 10	Month 36	Month 1	Month 10	Month 36
NC-1	27.4	31.4	32.4	4311.8	4569.5	4524.9
NC-2	30.4	34.8	35.2	4468.2	4688.6	4618.3
SFC-1	29.8	34.2	34.8	4644.8	4746.6	4758.8
SFC-2	29.8	34.5	34.8	4432.6	4668.4	4672.9
FAC	29.2	33.8	33.8	4484.3	4651.2	4594.2
BFSC	31.4	35	35.6	4641.1	4737.1	4769.5

Table 9. *Capillary water absorption coefficient and water absorption values of the concretes.*

Concrete Groups	Capillary water absorption coefficient x10^{-3} (cm/$s^{1/2}$)		Water absorption (%)	
	Month 1	Month 36	Month 1	Month 36
NC-1	0.889	0.112	3.7	0.4
NC-2	0.856	0.155	3.5	0.78
SFC-1	0.619	0.36	2.7	1.12
SFC-2	0.695	0.39	2.9	0.81
FAC	0.846	0.212	3.6	0.56
BFSC	0.64	0.234	2.7	1.15

Table 10. *Carbonation thickness of the concretes at month 36.*

Sample name	Time (Month)	Carbonation thickness (cm)
NC-1	36	0.53
NC-2	36	0.498
SFC-1	36	0.268
SFC-2	36	0.284
FAC	36	0.359
BFSC	36	0.349

Research Article | Submit Manuscript

Turkish Journal of Materials

Assessments of Tritium Concentration in the Some Water Samples around Rize

Serdar Dizman[1], Çiğdem Fındıklı Kağanoğlu[1], Neslihan İpek[1], Recep Keser[1,*]

[1]Recep Tayyip Erdoğan University, Faculty of Arts and Sciences, Department of Physics, Turkey

Published: 09.03.2018

Turk. J. Mater. Vol: 3 No: 1 Page: 53-57 (2018) ISSN: XXXX-YYYY

SLOI: http://www.sloi.org/sloi-name-of-this-article

*Correspondence E-mail: recep.keser@erdogan.edu.tr

ABSTRACT The aim of this study is to determine tritium levels in the seawater of Fırtına and Hemşin in Rize region, and along the coastline where these two rivers flow into. Sampling process was examined by applying ASTM D4107-08 method. Experimental studies were conducted by using scintillation device. Sampling coordinates were recorded by Magellan Explorist 510-GPS. After having collected 26 samples from Fırtına River, 23 samples from Hemşin River, and 28 samples from the seawater along the coastline, tritium concentration were calculated for 77 samples in total. Minimum detectable activity concentration (MDC) was determined as 1.36 Bq/L. The average tritium activity concentrations for Fırtına, Hemşin Rivers water samples and seawater samples for average tritium activity concentrations which were determined by liquid scintillation counting system were calculated as 2.666±1.136 Bq / L, 2.298±1.111 Bq / L and 1.874±1.161 Bq / L respectively. 2 water samples from Fırtına River, 6 water samples from Hemşin River, and 8 water samples taken from the seawater along the coastline were lower than MDC.

Keywords: Radioactivity, Tritium, LSC.

Cite this article: S. Dizman, Ç.F. Kağanoğlu, N. İpek, R. Keser. Assessments of Tritium Concentration in the Some Water Samples around Rize. Turk. J. Mater. 3(1) (2018) 53-57.

1. INTRODUCTION

Tritium (^{3}H) is a radiogenic form of hydrogen, used in research, nuclear power plants (NPP). Tritium has a half-life of 12.3 years and decays to ^{3}He with emission of a low-energy beta particle with maximum energy of 18.6 keV [1]. Tritium is produced naturally by cosmic ray interactions with hydrogen in the upper atmosphere and transfers to the troposphere. The environmental levels of this radionuclide were raised during nuclear weapon tests [2-6].

Once released to the atmosphere, inorganic tritium is rapidly oxidised to tritiated water (HTO). HTO can enter the human body by inhalation, absorption through the skin or ingestion of food and drinking water [7–9]. In the body, HTO is mixed rapidly with extracellular and intracellular tissue water, with a fraction replacing the hydrogen bound in organic molecules. Therefore, monitoring the internal exposure to HTO is important. HTO is one of the tritium forms that are harmful for humans, and it causes the most harm after internal exposure [10, 11].

Currently, there is no NPP in Turkey; however, agreements have been signed for the installation of an NPP. This NPP will be a pressurized water reactor type, scheduled to be in operation in 2019 [12].

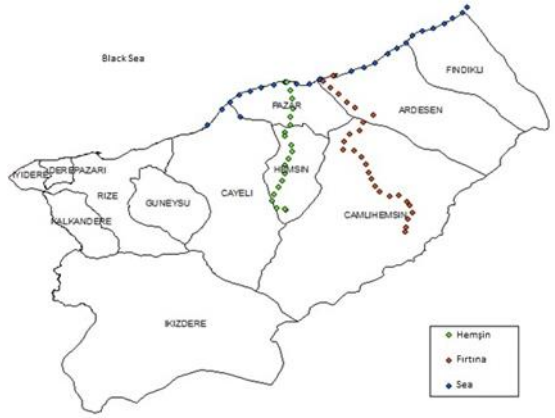

Figure 1. *Location of sampling regions.*

The aim of this study is to determine tritium levels in the water of Fırtına and Hemşin in Rize region, and along the coastline where these two rivers flow into. These results of this study will be used as baseline data for dose assessment of the regions when an unexpected tritium release occurs.

2. EXPERIMENTAL

Rize, which was selected as the pilot region, is a province of northeast Turkey, on the eastern Black Sea coast. Rize lies between latitudes of 40° 20' and 41° 20' N and longitudes of 40° 22' and 41° 28' E. Rize has a catchment area of 3920 km^2. It is on the north side of the range of mountains that runs along the Black Sea coast. Summers are cool (average 22°C), winters are warm (average 7°C), and it is wet all year. The population of Rize is 331,041 people [13].

Two large rivers (Fırtına and Hemşin) of Rize province water samples and seawater tritium values of samples (Fig. 1) were investigated by using LSC (Liquid Sintillation Counter) with ASTM D4107-08 method. About 500 mL of water sample was collected in a polyethylene bottle. The samples were treated rapidly to avoid unexpected contamination. Interferences during the counting such as quenching reduce the efficiency of detection. Therefore, a distillation process is usually applied to the sample to prevent quenching.

The background tritium concentration in the samples is relatively low [7, 14, 15] and hence sample preparation is needed. About 25 mL of water sample was added to 1.25 mg active charcoal, shaked vigorously for about 30 sec, and then filtered to obtain a clear filtrate. Then the filtrate was distilled. Distillation removes color but not all chemical impurities. These impurities react with scintillation liquid and cause luminescence. To remove luminescence, the samples had to be stored in a scintillation vial for 2–5 days in an opaque place or container before the measurement [4]. 10 ml of distilled sample was given into a measuring plastic vial (Zinsser Analytics, 20 ml), and scintillation cocktail (Ultima Gold LLT, Perkin Elmer Inc.) was added up to total volume of 20 ml. The plastic vials do not include ^{40}K, so they are more suitable for lower background levels and higher counting efficiency as compared with glass vials. Also, the vials were shaken for about one minute in order to make homogeneous solutions. Besides, the vials were cleaned outside with ethanol before placing them into the counter to prevent contamination.

A background sample was prepared by using twice-distilled groundwater with a low tritium concentration. The measurements were performed with a low-level liquid scintillation counter (Perkin Elmer Tricarb 2910 TR). The measurement time was set to 75 min × 10 times to evaluate the detection uncertainty and minimum detectable concentration (MDC). The measurement uncertainty was evaluated at the 95 % confidence level. The MDC for this method was calculated using Equation (1) [16].

$$\mathrm{MDC} = \frac{16.7x3.29\sqrt{cpm_b.t_s.\left(1+\frac{t_s}{t_b}\right)+3}}{\epsilon.t_s.V} \quad (1)$$

where cpm_b is the count rate of the background (cpm), t_s is the counting time of the sample (minute), t_b is the counting time of the background (minute), ε is the efficiency and V is the sample volume (liter).

Table 1. *Measurement results for samples spiked with different concentrations of a certified standard tritium source.*

Sample name	Spiked Activity (Bq L^{-1})	U[a] (%)	Measured activity (Bq L^{-1})	U[a] (%)	Relative bias (%)
HAS[b]	4.84E + 06	3.2	4.75E + 06	5.7	1.9
MAS[c]	4.02E + 03	3.2	3.77E + 03	5.9	6.2
LAS[d]	1.55E + 01	3.2	1.45E + 01	6.3	6.5

[a]Relative expanded standard uncertainty (k = 2).
[b]High-activity tritium sample.
[c]Medium-activity tritium sample.
[d]Low-activity tritium sample.

To verify this analysis method, three samples spiked with different levels of a certified standard tritium source (Eckert & Ziegler, P.O. No.: P700723, Source No.: 1676–44) were prepared and measured. The spiked and the measured activities are given in Table 1. Measurements were made at a 10:10 mixing ratio of the samples and the scintillation cocktail.

Table 2. *Tritium concentration and altitude information in Fırtına river water samples.*

Sample Code	Altitude of Sampling Point (m)	Tritium Concentration (Bq / l)
N1	2268	2.740±1.28
N2	2200	<MDC
N3	1945	2.409±0.921
N4	1754	2.075±1.241
N5	1585	1.941±1.381
N6	1492	1.874±1.162
N7	1379	<MDC
N8	1173	1.740±1.271
N9	1032	2.141±1.111
N10	1043	2.744±1.112
N11	782	3.145±1.112
N12	696	3.413±1.112
N13	590	2.744±1.112
N14	551	3.011±1.112
N15	518	2.610±1.112
N16	289	3.078±1.112
N17	282	3.346±1.112
N18	222	3.413±1.112
N19	181	2.543±1.112
N20	148	2.677±1.112
N21	124	3.279±1.112
N22	109	2.744±1.112
N23	70	3.011±1.112
N24	47	1.874±1.111
N25	24	2.476±1.112
N26	0	2.944±1.288
Maximum		3.413±1.112
Minimum		1.740±1.271
Average		2.666±1.136

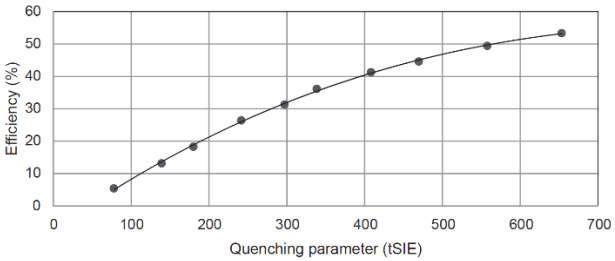

Figure 2. *Quench curve for tritium.*

A quenching calibration curve method was applied to determine the detection efficiency. Ten standard tritium samples with different quenching levels were prepared. The same tritium concentration was used in all the samples. To obtain different quenching effects, various volumes of the quenching agent (carbon tetrachloride) were added into vials. Then, vials were counted in the tritium (0–18.6 keV) counting windows, and the quench curve (Figure 1) of tritium was obtained by using the quenching parameter (tSIE).

Table 3. *Tritium concentration and altitude information in Hemşin river water samples.*

Sample Code	Altitude of Sampling Point (m)	Tritium Concentration (Bq / l)
P1	1165	<MDC
P2	1130	2.476±1.257
P3	967	<MDC
P4	818	4.417±1.242
P5	809	2.677±1.381
P6	688	3.346±1.163
P7	701	2.610±1.305
P8	580	1.606±1.271
P9	432	2.409±1.111
P10	356	<MDC
P11	318	2.476±1.112
P12	259	<MDC
P13	438	2.075±1.111
P14	164	2.543±1.112
P15	140	2.075±1.111
P16	135	2.141±1.111
P17	124	2.409±1.111
P18	109	<MDC
P19	70	2.476±1.112
P20	67	<MDC
P21	39	2.275±1.111
P22	11	2.543±1.112
P23	0	2.075±1.111
Maximum		4.417±1.242
Minimum		1.606±1.271
Average		2.298±1.111

Table 4. *Tritium concentration in seawater samples.*

Sample Code	Tritium Concentration (Bq / l)
D1	2.409±1.288
D2	1.740±1.257
D3	<MDC
D4	<MDC
D5	2.275±1.381
D6	2.141±1.162
D7	1.874±1.305
D8	3.681±1.272
D9	2.008±1.111
D10	<MDC
D11	<MDC
D12	<MDC
D13	<MDC
D14	<MDC
D15	2.128±1.111
D16	2.744±1.112
D17	2.075±1.111
D18	2.128±1.111
D19	1.941±1.111
D20	1.606±1.111
D21	2.208±1.111
D22	1.472±1.111
D23	1.807±1.111
D24	1.740±1.111
D25	<MDC
D26	2.008±1.111
D27	1.807±1.111
D28	1.807±1.111
Maximum	3.681±1.272
Minimum	1.472±1.111
Average	1.874±1.161

3. RESULTS

Table 2-4 shows the results of tritium concentration for the water samples taken along the Fırtına and Hemşin River waters and the coastline where these rivers emanate.

The average tritium concentration for 26 samples taken from Fırtına river was calculated as 2.666 ± 1.136 Bq / L (22.593 ± 9.627 TU). The maximum tritium concentration was found to be of 3.413 ± 1.112 Bq / L (28.924 ± 9.424 TU) with sample code N-12 and N-18. The lowest tritium concentration was found to be 1.74 ± 1.271 Bq / L (14.746 ± 10.771 TU), with sample code N-8 with 1173 m peak at 45.35807K - 06.76575D coordinates. Two samples were under the MDC.

The mean tritium concentration for 23 samples taken from Hemşin river was calculated as 2.298 ± 1.111 Bq / L (19.475 ± 9.415 TU). The highest tritium concentration was found to be 4.417 ± 1.242 Bq / L (37.432 ± 10.525 TU), with sample code P-4 with 818 m at 45.34244K-06.56770D coordinates. The lowest tritium concentration was found to be 1.606 ± 1.271 Bq / L (13.610 ± 10.771 TU), with sample code P-8 with a peak at 45.40544K -

06.58703D at 580 m. Six samples were under the MDC. The average tritium concentration for 28 samples taken from sea water samples was calculated as 1.874 ± 1.161 Bq / L (15.881 ± 9.839 TU). The highest concentration of tritium was found to be 3.681 ± 1.272 Bq / L (31.195 ± 10.780 TU) at 45.58654K-06.52483D, with sample code D-8. The lowest tritium concentration was found to be 1.472 ± 1.111Bq / L (12.475 ± 9.415 TU) at 45.68705K - 06.77067D, with sample code D-22. 8 samples were under the MDC.

Table 5. *The concentrations of tritium in water samples from Turkey and other study areas.*

Country	Tritium Concentration (Bq / l)	Sample Type	Reference
Japan (North Island)	2.42 ± 0.81 Bq/L (20.48±6.85 TU)	River water	[18]
Japan (South Island)	1.00 ± 0.36 Bq/L (8.46±3.05 TU) (20.31-134.56 TU)	River water	[18]
Spain	3.6±0.6 Bq/L (30.47±5.08 TU) (18.7 TU)	River water	[17]
India	0.51±0.04Bq/L (4.34±0.34 TU)	River water (Varahi)	[20]
India	0.66±0.09 Bq/L (5.61±0.84 TU)	River water (Markandeya)	[20]
Finland	0.92 Bq/L (7.8 TU)	Sea water	[19]
Finland	0.60 Bq/L (5.08 TU)	River water	[19]
Ireland	0.9-2.4 Bq/L (7.62-22.17 TU)	Sea Water	[21]
Turkey	1.64±0.94 Bq/L (13.88±7.95 TU)	River water (Büyükdere)	[25]
Turkey	1.72±0.94 Bq/l (14.56±7.95 TU)	River water (İkizdere)	[25]
Turkey	2.66±1.13Bq/l (22.59±9.62 TU)	River water (Fırtına)	Present Study
Turkey	2.29±1.11Bq/L (19.48±9.42 TU)	River water (Hemşin)	Present Study
Turkey	2.29±1.11Bq/L (19.48±9.42 TU)	Sea Water	Present Study

Totally 16 of 77 water samples were found to be below the MDC as a result of tritium concentration analysis. The concentration of tritium in Fırtına river water was higher than in Hemşin river water.

There are many studies of tritium activity levels in river and sea waters of different parts of the world. In order to be able to compare the present work, the average or variation values of the tritium concentration of some of these studies are given in Table 5. The results obtained in the present study are much lower than the results obtained from the river water samples of Spain [17] while the Japan (North Island) river water samples [18] were in close range with the obtained results. As can also be seen from Table 4. Fırtına and Hemşin river water samples have higher concentrations of tritium than Japan (South Island), Finland, Indian, Ireland, French river water samples [18-24].

4. CONCLUSION

Tritiated water concentrations were measured in 2 rivers and Sea water located in the northeast part of Turkey, Rize that were not directly influenced by the releases from any nuclear facilities. The average and the maximum tritium concentration in the water samples of 77 in the study area region was 2.279±1.136 Bq L^{-1}, 4.417± 1.242 Bq L^{-1}, respectively. About 21 % of the results are below the MDC (1.36 Bq L^{-1}). The measured values are lower than those in Japan (North Island) and Spain, but higher than those in Japan (South Island), India, Ireland, Finland. This indicates that environmental regions are important factors. Tritium continues to be a useful tracer in a post nuclear leak. Considering low concentrations in precipitation, the absence of the tritium transient allows for direct assessment of dwelling times by comparing precipitation and river water tritium concentrations. Briefly, the results of this study will be used as baseline data for dose assessment of the regions when an unexpected tritium release occurs.

Acknowledgement

This study was supported by the Recep Tayyip Erdogan University Scientific Research Projects Department (project no. 2014.102.01.01).

References

[1] UNSCEAR. Sources and effects of ionising radiation: sources and biological effects: report to the General Assembly with annexes. New York: United Nations Scientific Committee on the Effects of Atomic Radiation (1982).

[2] S. Kaufman, W. Libby. The natural distribution of tritium. Phys. Rev. 93 (1954) 1337–1344.

[3] S. Okada, N. Momoshima. Overview of tritium – characteristics, sources, and problems. Health Phys. 65 (1993) 595–609.

[4] M. Puhakainen, T. Heikkinen. Tritium in the urine in Finnish people. Radiat. Prot. Dosimetry. 128 (2008) 254–257.

[5] UNSCEAR. Sources, effects and risks of ionizing radiation: report to the general assembly with annexes. New York: United Nations Scientific Committee on the Effects of Atomic Radiation; (1988).

[6] F. Eyrolle, L. Ducros, S.L. Dizès, K.B.-Seiller, S. Charmasson, P. Boyer, C. Cossonnet. An updated review on tritium in the environment. J. Environ. Rad., 181 (2018) 128-137.

[7] P. Belloni, G.F. Clemente, S. Di Pietro, G. Ingrao. Tritium levels in blood and urine samples of the

members of the Italian general population and some exposed subject. Radiat. Prot. Dosimetry. 4 (1983) 109–113.
[8] C.N. Cawley, B.A. Lewis, L.A. Cannon. Possible parameters in the urinary excretion of tritium. Trans. Am. Nucl. Soc. 50 (1985) 39–44.
[9] R.L. Hill, J.R. Johnson. Metabolism and dosimetry of tritium. Health Phys. 65 (1993) 628–647.
[10] ICRP. Protection of the public in situations of prolonged radiation exposure. ICRP Publication 82, Ann. ICRP 29. Ottawa: International Commission on Radiological Protection (1999).
[11] E.L. Etnier, C.C. Travis, D.M. Hetrick. Metabolism of organically bound tritium in man. Radiat. Res. 100 (1984) 487– 502.
[12] DNEPI. Nükleer santraller ve ülkemizde kurulacak nükleer santrale ili¸skin bilgiler. Department of nuclear energy project implementation, publication no:2. Republic of Turkey: Ministry of Energy and Natural Resources (2012).
[13] ABPRS. Address based population registration system. Turkey: Turkish Statistical Institute (2017).
[14] N. Momoshima, Y. Nagasato, Y. Takashima. A sensitive method for the determination of tritium in urine. J. Radioanal. Nucl. Chem. Lett. 107 (1986) 353–359.
[15] Y. Ujeno, K. Yamamoto, T. Aoki, N. Kurihara. Tritium content in tissue free water of Japanese bodies. Radiat. Prot. Dosimetry. 16 (1986) 181–183.
[16] L.A. Currie. Limits for qualitative detection and quantitative determination. Anal. Chem. 40 (1968) 586–593.
[17] M. Palomo, A. Peñalver, C. Aguilar, F. Borrull. Tritium activity levels in environmental water samples from different origins. Appl. Radiat. Isot. 65(9) (2007) 1048-56.
[18] N. Momoshima, T. Kaji, I.T. Poppy, N. Inoue, Y. Takashima. Tritium concentrations of river water on northern and southern islands of Japan. Journal of Radioanalytical and Nuclear Chemistry, 150 (1991) 163.
[19] K. Marianna, D. Alena, Tritium in the Water Environment of Baltic Sea basin. 2010 International Conference on Biology, Environment and Chemistry (IPCBEE) IACSIT Press, Singapore, 1 (2011).
[20] L. Ducros, F. Eyrolle, C. D. Vedova, S. Charmasson, M. Leblanc, A. Mayer, M. Babic, C. Antonelli, D. Mourier, F. Giner, Tritium in river waters from French Mediterranean catchments: Background levels and variability, Science of The Total Environment, 612, (2018), 672-682.
[21] Ravikumar P. Somashekar RK. Environmental tritium (^{3}H) and hydrochemical investigations to evaluate groundwater in Varahi and Markandeya river basins, Karnataka, India. J. Environ. Radioact. 102(2) (2011) 153-62.
[22] P.A. Harms, A. Visser, J. E. Moran, B.K. Esser, Distribution of tritium in precipitation and surface water in California, Journal of Hydrology, 534 (2016), 63-72.
[23] A. Cauquoin, P. Jean-Baptiste, C. Risi, É. Fourré, B. Stenni, A. Landais, The global distribution of natural tritium in precipitation simulated with an Atmospheric General Circulation Model and comparison with observations, Earth and Planetary Science Letters, 427 (2015) 160-170.
[24] L. Currivan, K. Kelleher, P. McGinnity, J. Wong and C. McMahon. A survay of tritium in Irish seawater. Radiologinal Protection Institute of Ireland, RPII 13/02 (2013) 30.
[25] N. İpek. Determination of the Tritium Level in Some Rivers and Sea Water Samples in Rize. Master Thesis. Recep Tayyip Erdogan University, Institute of Science and Technology, Rize, Turkey, (2015) 84.